European Polymer Journal 147 (2021) 110307

Contents lists available at ScienceDirect

European Polymer Journal

journal homepage: www.elsevier.com/locate/europolj

Comonomer effects on co-permeation of methanol and acetate in cation exchange membranes

Jung Min Kim, Bryan S. Beckingham *

Department of Chemical Engineering, Auburn University, Auburn AL 36849, United States

ARTICLE INFO

Keywords:
Permeability
Multicomponent transport
in situ ATR FTIR spectroscopy
Ion exchange membrane
PEGDA

ABSTRACT

Co-permeation in hydrated, dense polymer membranes is crucial to many applications from energy conversion (i.e. photoelectrochemical CO_2 reduction cells) to liquid separation (i.e. pervaporation), where such membranes are challenged with complex mixtures of species. For instance, a major challenge to the realization of efficient CO_2 reduction cells is the design of ion exchange membranes with sufficient conductivity and minimal permeation of CO_2 reduction products (e.g. methanol and acetate), such that understanding permeation and co-permeation behavior of these solutes in ion exchange membranes is needed. Previously, the transport behavior of Nafion® 117 and crosslinked cation exchange membranes prepared with poly(ethylene glycol) diacrylate (PEGDA, crosslinker) and 2-acrylamido-2-methyl-1-propanesulfonic acid (AMPS, sulfonated comonomer) to methanol and sodium acetate was investigated and distinct changes in permeabilities of these membranes to sodium acetate was observed in co-permeation with methanol. To further investigate this co-permeation behavior, we modify the PEGDA-AMPS structure by varying the negatively-charged AMPS content with three different comonomers, acrylic acid (AA, n = 0), 2-hydroxylethyl methacrylate (HEMA, n = 1), and poly(ethylene glycol) methacrylate (PEGMA, n = 5), where n represents the number of ethylene oxide repeat units in each comonomer. While the observed permeability to sodium acetate in co-permeation with methanol was increased for membranes with comonomers with short pendant groups (PEGDA-AMPS/AA and PEGDA-AMPS/HEMA), it remained relatively consistent for PEGDA-AMPS/PEGMA membranes. While the underlying causes of this type of behavior remains unresolved, we propose a combination of assisted transport by methanol and disruption of electrostatic interactions by pendant ethylene oxide repeat units based on our experiments. Overall, such differences in transport behavior underscore the need for increased understanding of emergent co-permeation behavior in hydrated, dense polymer membranes.

1. Introduction

Dense polymeric membranes are semipermeable membranes that can promote selective transport of certain small molecules over others, leading to separation based on polymer properties such as internal morphology, hydrophobicity, ion content, etc. [1–3]. Ion exchange membranes are a unique type of dense membranes that can provide additional selectivity toward charged ions through repulsive electrostatic interactions with their covalently attached charged moieties [4–6]. With these properties, ion exchange membranes are utilized in numerous energy applications, such as direct methanol fuel cells (DMFC [7]), vanadium redox flow batteries [8], and solar fuels devices [9]. While a typical goal of ion exchange membrane research is enhanced ionic conductivity at relatively low swelling [10], requirements of each application are different. For instance, one of the major membrane requirements for DMFC is the minimization of methanol permeation as it reduces overall performance [7,11]. Alternatively, a photoelectrochemical CO_2 reduction cell (PEC-CRC) is a solar fuels device that reduces CO_2 into valuable products, including methanol and acetate, at the cathode [12,13]. A crucial membrane requirement for PEC-CRC is to minimize the permeation of CO_2 reduction products such as these from the complex mixtures of simultaneously produced reduction products [9,13–15]. Research on CO_2 reduction catalysts for selective CO_2 reduction is an active field of research, which can be found elsewhere [16,17]. Favorably, PEC-CRC does not require membranes with high ionic conductivity as these devices can be operated at relatively low current, which creates an opportunity to trade ionic conductivity for more controlled transport behavior by manipulating the chemistry and

* Corresponding author.
E-mail address: bsb0025@auburn.edu (B.S. Beckingham).

https://doi.org/10.1016/j.eurpolymj.2021.110307
Received 12 November 2020; Received in revised form 8 January 2021; Accepted 19 January 2021
Available online 1 February 2021

morphology of the polymer matrix [9,13,18].

Transport of small molecules through dense membranes is often described by the solution-diffusion model [3], which describes solutes absorption into the membrane and diffusion through the membrane fractional free volume in the direction of the chemical potential gradient:

$$P_i = D_i K_i \quad (1)$$

where P_i is the membrane permeability to solute i, D_i is the membrane diffusivity to solute i, and K_i is the membrane solubility to solute i. In the case of multi-solute transport, membrane permeability to each solute is expected to be reduced due to competitive sorption [19]. However, emergent multi-solute transport behavior has been observed such that membrane permeability to acetate was significantly increased in co-permeation with methanol in the commercial cation exchange membrane, Nafion® 117 [20]. Recently, we observed analogous behavior in isotropic cation exchange membranes prepared by free radical UV photocrosslinking of poly(ethylene glycol) diacrylate (PEGDA, n = 13) and 2-acrylamido-2-methylpropane sulfonic acid (AMPS, bound anion) [21]. Previously, to rationalize this observed emergent transport behavior, we proposed a major cause for this transport behavior is the shielding of electrostatic repulsion, where transporting methanol molecules interfere with the electrostatic repulsion between membrane-bound sulfonates and transporting acetate molecules [20,21]. Here, we further investigate multi-solute transport behavior in cation exchange membranes by modifying the internal structure of crosslinked PEGDA-AMPS membranes [21,22]. We vary the AMPS content with charge-neutral pendant comonomers of different chain lengths, namely acrylic acid (AA, n = 0 [23]), 2-hydroxyethyl methacrylate (HEMA, n = 1), and poly(ethylene glycol) methacrylate (PEGMA, n = 5) [24]. Membranes are characterized for in-plane ionic conductivity and water uptake in addition to investigating the effect of comonomer chains in multi-solute transport of methanol and acetate by measuring diffusive permeabilities of methanol and acetate by themselves and in co-permeation.

2. Experimental methods

2.1. Materials

Methanol (99.8%) was purchased from British Drug House (BDH®) Chemicals (Poole, UK) and sodium acetate (99%) was purchased from ACS Chemical Inc. (Point Pleasant, NJ). Poly(ethylene glycol) diacrylate (PEGDA, n = 13), 2-acrylamido-2-methyl-1-propanesulfonic acid (AMPS, 99%), and 2-hydroxyethyl methacrylate (HEMA, n = 1) were purchased from Sigma-Aldrich Chemicals (St. Louis, MS). Acrylic acid (AA, n = 0) was purchased from Alfa Aesar (Haverhill, MA). Poly (ethylene glycol) methacrylate (PEGMA, n = 5) was purchased from Polysciences Inc. (Warrington, PA). 1-Hydroxyl-cyclohexyl phenyl ketone (HCPK, photoinitiator) was purchased from Tokyo Chemical Industry (Japan). All water used in this investigation was Type-1 deionized water produced by a Waterpro BT Purification System from Labconco® (18.2 mΩ cm at 25 °C, 1.2 ppb TOC) (Kansas City, MO).

2.2. PEGDA-Comonomer and PEGDA-AMPS/Comonomer membrane polymerization

The detailed procedure for crosslinked PEGDA-based films is described elsewhere [7,21,22,24–26]. A total of 6 new compositionally dissimilar membranes were prepared by free radical UV photocrosslinking of prepolymerization mixtures (solutions of solvent, monomer, and initiator), as shown in Fig. 1 and Table 1. All membranes contain 67 mol% of PEGDA (n = 13) with the remaining 33 mol% varied between AMPS and one of the three comonomers; AA (n = 0), HEMA (n = 1), and PEGMA (n = 5).

In addition to these monomers, each prepolymerization mixture contained 20 wt% of water and 0.1 wt% of HCPK as a free radical photoinitiator, as shown in Table 1. Each prepolymerization mixture was sonicated for 30 min to achieve a homogeneous solution and placed in between two quartz plates (5 × 5 × 1/4″) separated by two spacers (305 μm). This setup was then placed inside a UV crosslinking oven, Spectrolinker™ XL-1500 from Spectroline (Westbury, NY), under 254 nm for 3 min at 3.0 mW/cm^2. All films with the thickness of the spacers

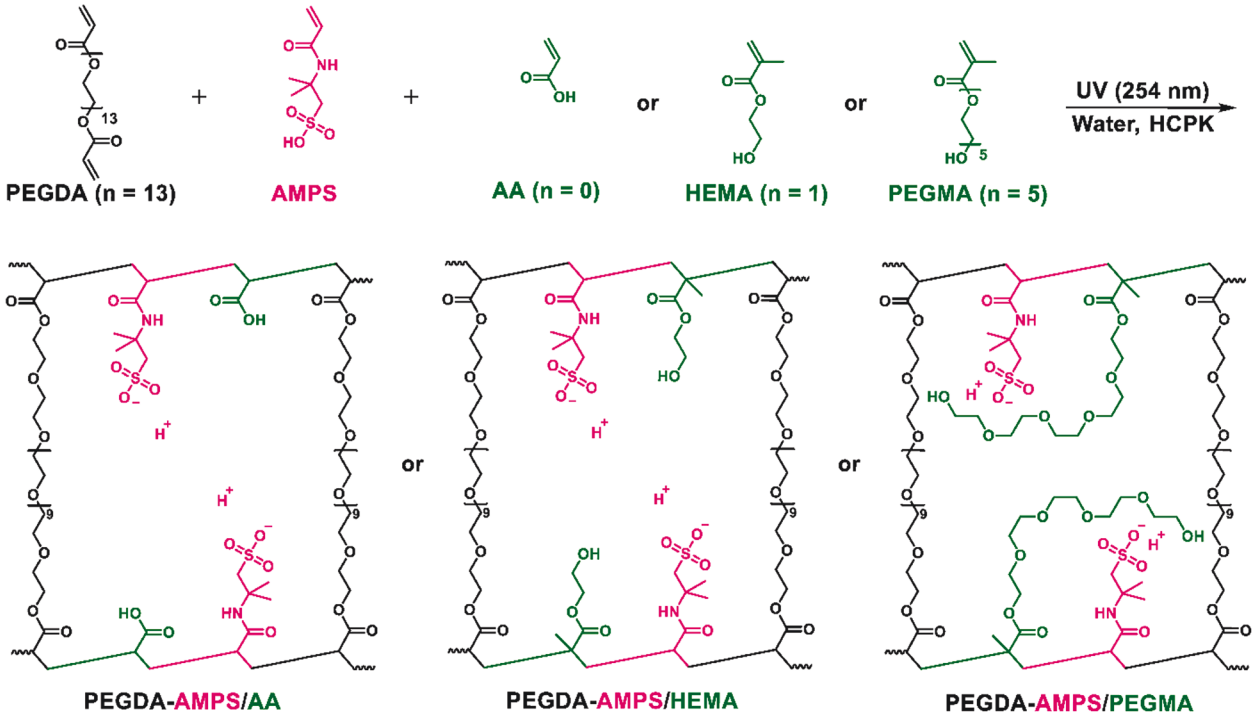

Fig. 1. Scheme of PEGDA-AMPS/AA, PEGDA-AMPS/HEMA, and PEGDA-AMPS/PEGMA membrane polymerization via free radical UV photopolymerization.

Table 1
Membrane properties from pre-polymerization mixtures.

	AMPS[a] (mol%)	Comonomer[b] (mol%)	PEGDA (g)	AMPS (g)	Comonomer (g)	Water (g)	HCPK (g)	IEC (meq/g dry polymer)[c]
PEGDA-	0	33	7.00	0.00	0.35	2.00	0.01	0.60
AMPS/AA	16.5	16.5	7.00	0.50	0.17	2.00	0.01	0.60
PEGDA-	0	33	7.00	0.00	0.63	2.00	0.01	0.00
AMPS/HEMA	16.5	16.5	7.00	0.50	0.31	2.00	0.01	0.31
PEGDA-	0	33	7.00	0.00	1.38	2.00	0.01	0.00
AMPS/PEGMA	16.5	16.5	7.00	0.50	0.69	2.00	0.01	0.30
PEGDA-AMPS*	33	0	7.00	1.00	0.00	2.00	0.01	0.60

* Previously reported by Kim et al.[21].
[a] AMPS = mol of AMPS/(mol of PEGDA + mol of AMPS + mol of comonomer) × 100%.
[b] Comonomer = mol of comonomer/(mol of PEGDA + mol of AMPS + mol of comonomer) × 100%.
[c] Theoretical IEC = (mmol of AMPS + mmol of AA)/(mass of PEGDA + mass of AMPS + mass of HEMA or PEGMA).

were carefully recovered and immersed in 1 L of water for 2 days before further use. The inclusion of AMPS chains in the polymer network has been verified by ATR-FTIR; see Supporting information Figure S1 [24,25,27]. Essentially complete conversion has been determined as the mass of polymer network-forming monomers in the prepolymerization mixtures accords with the mass of the films after vacuum drying at 50 °C following 5 days of swelling in DI water within ~ 99% [21,22,24,28].

2.3. Ionic conductivity measurements

In-plane conductivity of all films was measured using a conventional two-probe electrochemical impedance spectroscopy technique (EIS, frequency: 10 Hz-1 MHz, AC voltage: 10 mV) employed with a Gamry Interface 1000 potentiostat [21]. Two platinum wires, as working and counter electrodes, are placed over a glass slide spaced by 0.5 cm, L. A rectangular section of film (length: >1.0 cm, width: 0.5 cm, W) was cut and placed over two platinum wires. An identical glass slide was placed over the film and a vial (~33 g) was placed over the setup to ensure good contact. EIS was performed after the open circuit potential stabilized. EIS data was analyzed in Gamry Echem Analyst software and the resistance, R (Ω), was obtained from a Nyquist plot. The ionic conductivity, σ, was measured as follows:

$$\sigma = \frac{L}{RWT} \tag{2}$$

where L, W, and T are the distance between two electrodes, the width, and the thickness of the film, respectively.

2.4. Water content

Water uptake was measured gravimetrically. A 0.75-inch diameter hole punch was used to cut 3 hydrated films. The mass of the hydrated films, W_s, was measured after quickly blotting with tissue paper. The film was then dried under vacuum at 50 °C for 24 h and the mass of the dried film, W_d, was measured [20]. The water uptake, ω_w, was measured as via Eq. (3), where W_s is the mass of the swollen films and W_d is the mass of the dried film.

$$\omega_w = \frac{W_s - W_d}{W_d} \cdot 100\% \tag{3}$$

2.5. Solute permeability

The detailed experimental method for measuring solute permeability has been thoroughly discussed elsewhere [21,29]. Briefly, methanol and sodium acetate permeabilities in hydrated films were measured using a temperature jacketed custom-built diffusion cell coupled with an in-situ ATR-FTIR probe (Mettler-Toledo ReactIR™ 15 with a shallow tip 9.5 mm DSun AgX DiComp probe) to detect the evolving methanol and sodium acetate concentration in the receiver cell via absorbance. The feed cell was initially filled with either 1 M methanol, 1 M sodium acetate, or a binary mixture of 1 M methanol and 1 M sodium acetate, while the receiver cell was initially filled with water. The time-resolved concentrations of each solute were measured from the time-resolved FTIR spectra acquired in the receiver cell and fitted to Yasuda's model to calculate the permeability [1,2]. The osmotic flow of water from receiver cell to the feed cell was neglected in this study as the difference due to osmotic flow was within the experimental error for identical solutions in Nafion® 117 [20].

3. Result and discussion

A series of PEGDA-Comonomer membranes and PEGDA-AMPS/Comonomer membranes were prepared using free radical UV photopolymerization and used as model membranes to investigate the effect of comonomers on solute and multi-solute transport behavior of cation exchange membranes. Water uptake, ionic conductivity, and diffusive permeabilities of PEGDA-AMPS cation exchange membranes acquired in a previous study are leveraged towards understanding the transport behavior of the membranes prepared here [21]. Each comonomer has a pendant chain with a terminal alcohol moiety, but a different number of pendant PEG repeating units—AA (n = 0), HEMA (n = 1), and PEGMA (n = 5)—impacting both the side chain length and the overall poly (ethylene oxide) (PEO) content in the resulting polymer network. This structural variation is important to note as it influences membrane properties such as water uptake, and the probability of interactions between neighboring and other repeat units (chain-chain interactions) [21–24]. Moreover, variation between AMPS-to-comonomer content impacts the overall PEO and membrane-bound sulfonate content, which in turn influences the network structure, ion exchange capacity (IEC), ionic conductivity, and water uptake of the membranes. We note here that as the comonomer pendant chain length of AA and HEMA are relatively short, they are less likely to interact with neighboring AMPS chains. In contrast, the considerably longer PEGMA chain is more likely to interact with neighboring AMPS repeat units, and thereby more likely to impact the electrochemical gradient inside the membrane during ionic transport through these films. Ultimately, we believe these differences in side-chain length play a key role in the observed emergent transport behavior, a point we will return to in the discussion. In the context of this varied polymer membrane chemistry and potential structural changes, we evaluate the similarities and differences in transport-related physiochemical properties and transport behavior.

3.1. Water uptake and ionic conductivity of membranes

Membrane water uptake was measured gravimetrically with results shown in Fig. 2(A); see Supporting information Table S1. Water uptakes of PEGDA-AA, PEGDA-HEMA, and PEGDA-PEGMA remained relatively constant, 69, 68, and 67%, respectively. Similar behavior has been observed by Sagle et al., where water uptakes of PEGDA-Comonomer

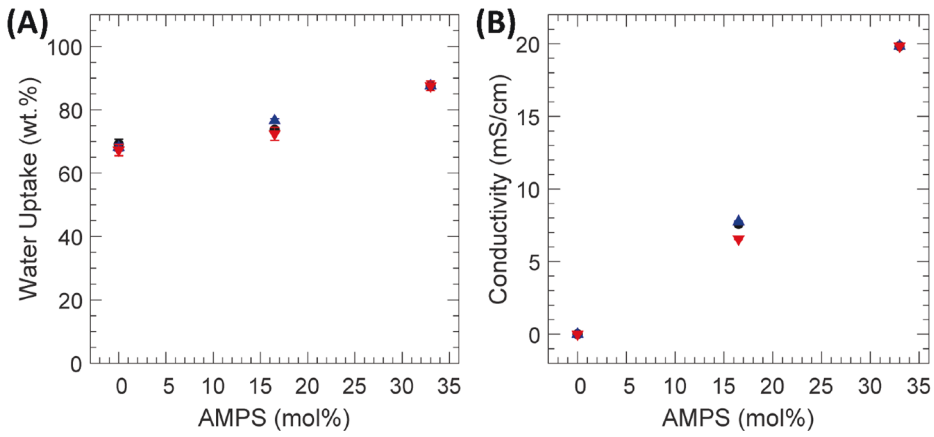

Fig. 2. (A) Water uptake and (B) ionic conductivity of AA-containing, ●, HEMA-containing, ▲, and PEGMA-containing,▼, films. Each data point is the average of 3 membranes with error bars corresponding to the standard deviation.

films prepared with different comonomers (AA, 2-hydroxyethyl acrylate (HEA), and poly(ethylene glycol) acrylate (PEGA)) were consistent for films prepared with less than 40 mol % of comonomer content [24]. Water uptakes of PEGDA-AMPS/Comonomer films were between those of PEGDA-Comonomer and PEGDA-AMPS within the same type of comonomer and PEGDA content. This is consistent with prior work where increasing content of ionogenic groups (and likely thereby the hydrophilicity) leads to increasing water uptake and often water-solubility of the linear (non-crosslinked) polymers [30–33]. The variation among films containing different comonomers were negligible such that the amount of fractional free volume among PEGDA-Comonomer films and among PEGDA-AMPS/Comonomer films are likely similar.

The ionic conductivity of the prepared membranes was measured yielding the results shown in Fig. 2(B); see Supporting information Table S1. Ionic conductivities of all PEGDA-Comonomer films which do not contain AMPS were negligible; on the order of 10^{-2} mS/cm for PEGDA-AA and 10^{-3} mS/cm for PEGDA-HEMA and PEGDA-PEGMA. Note, AA contains acidic groups, however the ionic conductivity of PEGDA-AA is negligible due to the weak acidic nature of the pendant carboxylic acid group [34]. All AMPS-containing films displayed ionic conductivities which increased with increasing AMPS content. Additionally, the ionic conductivities of PEGDA-AMPS/Comonomer films were analogous for films with the same AMPS content regardless of the comonomer; e.g. 8, 8, and 7 mS/cm with 16.5 mol% AMPS.

3.2. Single and Multi-solute permeability

The diffusive permeabilities of all prepared membranes to methanol and sodium acetate in single and co-permeation were measured in triplicate. Concentration versus time plots are shown in Fig. 3 for the PEGDA-AMPS/HEMA films from diffusion cell experiments with methanol, sodium acetate, and their binary mixture as a representative example of these experiments. Extracted permeability values using the Yasuda model [1,2]:

$$P_i = ln\left(1 - \frac{2c_{i,l}(t)}{c_{i,0}}\right)\left(\frac{-lV}{2At}\right) \quad (4)$$

where P_i is the membrane permeability to solute i, $c_{i,l}(t)$ is the concentration of solute i in receiver cell at time t, $c_{i,0}$ is the initial concentration of solute i in feed cell (1 M), l is the membrane thickness, and V is

Table 2
Diffusive permeabilities of PEGDA-AMPS/Comonomer membranes to methanol and sodium acetate in single and two-solute measurements.

		Single solute in feed cell		Both solutes in feed cell	
	AMPS (mol %)	Methanol ($\times 10^{-7}$ cm^2/s)	Sodium acetate ($\times 10^{-7}$ cm^2/s)	Methanol ($\times 10^{-7}$ cm^2/s)	Sodium acetate ($\times 10^{-7}$ cm^2/s)
PEGDA-AMPS/AA	0	9.9 ± 0.0	1.2 ± 0.0	10.5 ± 0.1	1.7 ± 0.0
	16.5	14.3 ± 0.2	1.4 ± 0.0	12.6 ± 0.7	2.1 ± 0.4
PEGDA-AMPS/HEMA	0	9.8 ± 0.1	1.0 ± 0.0	9.4 ± 0.4	1.6 ± 0.2
	16.5	13.7 ± 0.2	1.2 ± 0.0	12.2 ± 0.8	2.3 ± 0.2
PEGDA-AMPS/PEGMA	0	11.2 ± 0.3	1.4 ± 0.1	11.0 ± 0.1	1.6 ± 0.1
	16.5	13.1 ± 0.5	1.4 ± 0.1	12.7 ± 0.2	1.6 ± 0.2
PEGDA-AMPS	33*	15.1 ± 0.7	1.6 ± 0.4	14.5 ± 0.7	2.0 ± 0.3

* Previously reported by Kim et al.[21].

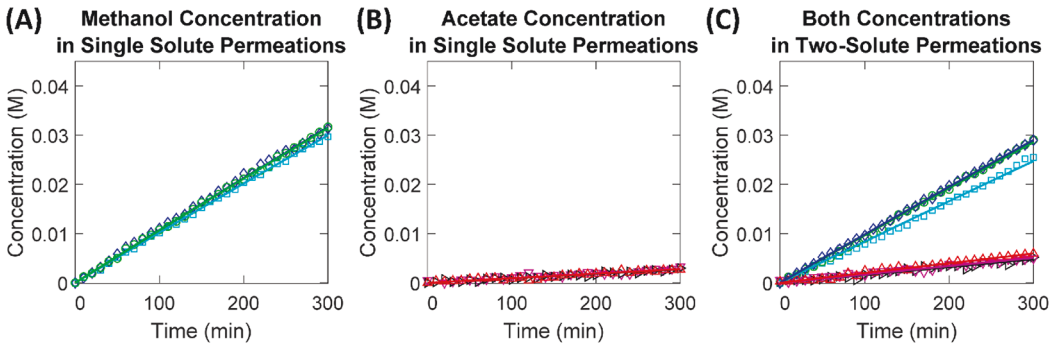

Fig. 3. Time-resolved solute concentration (A) for methanol, (B) for sodium acetate, and (C) for both methanol and sodium acetate in co-permeation where lines are fit of the Yasuda model. Only 10% of data are shown for clarity.

the volume of a half-cell (25 mL), A is the cross-sectional area of the orifice of half-cells (1.1423 cm^2). All permeability values are shown in Table 2 and Fig. 4. Overall, negligible membrane swelling is observed, where 16 out of 21 cases were within 2% change in normalized film thickness; see Supporting information Table S2. Slight deswelling (4–7% change in normalized film thickness compared to in DI water) was observed for PEGDA-PEGMA films in all cases, and for PEGDA-HEMA films in sodium acetate-containing transport experiments (see Table S2).

Generally, methanol permeabilities were larger than sodium acetate permeabilities by a factor of ~ 8. This behavior is partially due to diffusivity differences [7] as the kinetic diameter of methanol (3.6 Å [35]) is smaller than the hydrated diameters of dissociated ions, such as sodium ion (7.16 Å [36]) and acetate ion (7.44 Å [37,38]). In single-component permeation, permeability to methanol was increased with increasing AMPS content which also correlates to higher fractional free volume (FFV) within each membrane as indicated from water uptake [7]. Permeability to sodium acetate also increased with increasing AMPS content and water uptake. For sodium acetate this indicates the impact of increasing electrostatic repulsion between polymer-bound sulfonate anions and transporting acetate anions (which would hinder transport) was minor compared to the increased transport from higher FFV. To examine the effect of FFV on solute permeability more clearly, the co-efficient of variation (CV) was calculated for the ratios of water uptake to methanol permeability and water uptake to acetate permeability in single solute transport; see Supporting Information Table S3 for values. The CVs of both ratios were less than 11%, which indicates that water uptake is closely linked with the permeation of both solutes in these films. We also examined the effect of different comonomers on solute permeabilities by calculating the CV among PEGDA-Comonomer films and among PEGDA-AMPS/Comonomer films; see Supporting Information Table S4 for values. The CV of all single component permeabilities were also small (less than 7% except for acetate in PEGDA-comonomer films which was 11%) indicating that while differences in permeability were observed based on the membrane chemistry, the overall impact of the different comonomers was generally limited (but most pronounced for acetate in PEGDA-Comonomer films) in the context of deviation from the average single component permeabilities.

In co-permeation, methanol permeabilities were consistent with single component permeabilities. To examine the relative difference in methanol permeabilities from all films, the CV of the ratios between two component permeability over single component permeability were calculated; see Supporting Information Table S5. The CV of the ratios was relatively small (5.8%), corresponding to a small effect of co-permeating acetate on methanol transport. Particularly, methanol permeabilities of PEGDA-Comonomer films (PEGDA-AA, PEGDA-HEMA, and PEGDA-PEGMA) were consistent with those measured in single component permeation; where the differences were 6, 4, and 1%, respectively. This indicates the presence of co-permeating sodium acetate has a small-to-negligible impact on the permeation of methanol in these AMPS-free films. Alternatively, methanol permeabilities in PEGDA-AMPS/AA and PEGDA-AMPS/HEMA films were decreased by 14 and 12% in co-permeation with sodium acetate, indicating co-permeating sodium acetate has a much larger impact on methanol permeability in these AMPS-containing films. In all cases, one possible cause of this reduced methanol permeability is competitive transport [15,29,39,40], where the transport of a permeant (methanol) may be decreased in co-permeation due to competition with other permeants (acetate) for the fractional free volume necessary to perform diffusional jumps. We note, that while membrane swelling is a factor this behavior cannot be explained strictly through a swelling argument as PEGDA-AA films experienced slightly higher swelling (based on normalized film thickness, Table S2) with both solutes compared to solely methanol (1.01 vs 0.98), while PEGDA-HEMA films exhibit the opposite behavior (0.96 vs 0.98). On the other hand, the difference between one- and two-

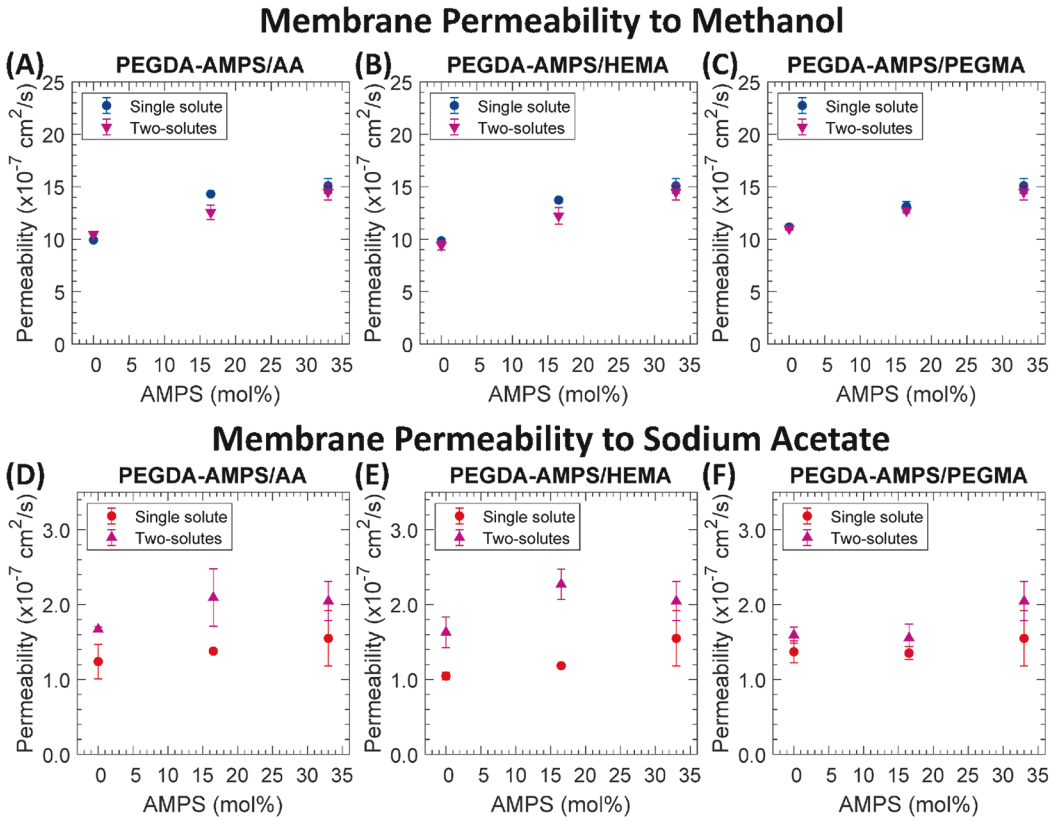

Fig. 4. (A-C) Methanol and (D-F) sodium acetate permeability in (A,D) PEGDA-AMPS/AA, (B,E) PEGDA-AMPS/HEMA, and (C,F) PEGDA-AMPS/PEGMA. Each data point is the average of 3 membranes with error bars corresponding to the standard deviation.

component permeability to methanol was relatively small, ~3%, in PEGDA-AMPS/PEGMA films, which also exhibited negligible change in swelling (0.94 vs 0.93 in normalized film thickness). As we noted above, the difference in co-transport behavior between PEGMA-containing films and other films may be examined and rationalized through the differing chain length of the comonomers and their impact on solutes permeating through the polymer film. The significantly longer ethylene oxide chain in PEGMA-containing films compared to AA- and HEMA-containing films, as shown in Fig. 1, may have more interactions with the permeants and thereby interfere with the other permeant-membrane interactions such as between permeants and the sulfonates on the AMPS chain end.

In co-permeation, sodium acetate permeabilities to all films were substantially increased (15 to 92%). To examine the relative difference in sodium acetate permeabilities from all films, the CV of the ratios between two component permeability over single component permeability were calculated; see Supporting Information Table S5. The CV of the ratios for acetate permeability was relatively large (17.4%), indicating that co-permeating methanol has a more significant impact on acetate permeation. One possible contribution to this behavior is assisted transport [20,21,29,41], where interactions with a fast-permeating co-permeant (methanol) facilitates diffusional jumps of the slower permeant (acetate) thereby increasing its observed permeability. However, this is likely not the only contributing phenomena as many other factors (hydration number of dissociated ions [42,43], feed concentration [20], degree of swelling, shielding of electrostatic repulsion [20,21], etc.) likely play a role in this transport behavior. However, we also note again that there is a distinct difference between the behavior based on the comonomer chain length. The increase in sodium acetate permeabilities of membranes prepared with shorter comonomers (AA and HEMA) was higher than those of membranes prepared with PEGMA, the longest. In PEGDA-Comonomer films, the increase in sodium acetate permeability in co-permeation was relatively large in PEGDA-AA and PEGDA-HEMA, 34 and 56%, respectively, while it was relatively small in PEGDA-PEGMA, 16%. This indicates the length of the pendant chain is likely a key factor where, for instance, a long pendant chain (PEGMA) may interfere with the assisted transport by methanol. Similarly, the increase in sodium acetate permeability in co-permeation was large in PEGDA-AMPS/AA and PEGDA-AMPS/HEMA, 52 and 92%, respectively, while it was relatively small in PEGDA-AMPS/PEGMA, 15%. A pictorial description of the interactions and transport within these films is shown in Fig. 5, where Fig. 5.(1) and Fig. 5.(3) depict acetate transport, Fig. 5.(2) and Fig. 5.(4) depict acetate and methanol co-transport. In particular, Fig. 5.(2) portrays how acetate transport could be assisted by co-permeating methanol in absence of long pendant chains and Fig. 5.(4) shows the effect of assisted transport being diminished by long pendant chains.

We also examined the difference in sodium acetate permeabilities in co-permeation among PEGDA-Comonomer films and among PEGDA-AMPS/Comonomer films by calculating the CVs; see Supporting Information Table S4 for values. The CV of sodium acetate permeabilities in co-permeation for PEGDA-Comonomer films was small (1.9%), while that for PEGDA-AMPS/Comonomer films was large (15.4%) with the permeability of PEGDA-AMPS/PEGMA film being significantly less than those of PEGDA-AMPS/AA and PEGDA-AMPS/HEMA. This signifies how the effect of different comonomer was most pronounced for acetate transport in AMPS-containing films. Focusing on films with shorter comonomers, AA and HEMA, the increases in acetate permeabilities in AMPS-containing films, PEGDA-AMPS/AA and PEGDA-AMPS/HEMA, were larger than AMPS-free films, PEGDA-AA and PEGDA-HEMA. Overall, this points to a distinct link between comonomer chain length and transport behavior as the difference in one- and two-component acetate permeabilities of films with longer comonomer (PEGMA) are small, while those of films with shorter comonomers (AA and HEMA,) are more significant. However, this is just one of many factors in manipulating transport and multicomponent transport in these and analogous films where more investigations are needed in order to further develop our understanding of these complex transport behaviors.

4. Conclusions

A series of PEGDA-Comonomer and PEGDA-AMPS/Comonomer membranes with varied AMPS to comonomer content were prepared. Water uptake and ionic conductivity were measured in addition to diffusive permeabilities to methanol and sodium acetate in both single and co-permeation. Emergent co-transport behavior is observed and attributed to both competitive and assisted transport effects that result from the combined impacts of membrane structure, species concentrations, ion hydration number, electrostatic repulsion, and swelling. The change in permeation behavior upon introduction of the co-solute was significantly reduced in PEGMA-containing films which we believe is a direct result of the longer pendant PEGMA chain interfering with the interactions between methanol and sodium acetate. While this behavior requires further study, this work highlights the role employing uncharged comonomers in ion exchange membranes can play in manipulating co-permeation behavior.

CRediT authorship contribution statement

Jung Min Kim: Conceptualization, Methodology, Investigation, Validation, Formal analysis, Writing - original draft, Visualization. **Bryan S. Beckingham:** Conceptualization, Methodology, Resources, Writing - review & editing, Supervision, Project administration, Funding acquisition.

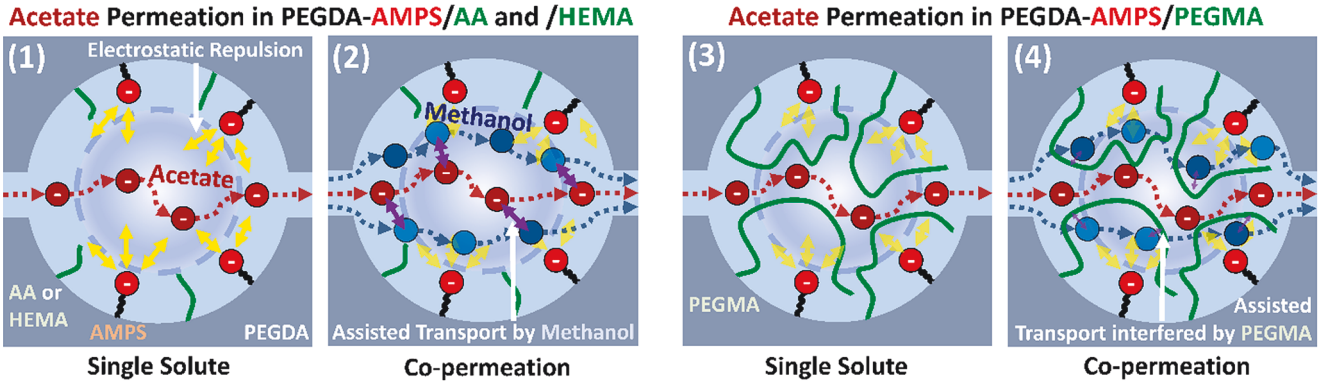

Fig. 5. A postulated acetate permeation in films with (1,2) shorter comonomers, AA and HEMA, and (3,4) a longer comonomer, PEGMA, where (2) co-permeating methanol assist acetate transport and (4) long PEGMA chain interfere the assisted transport.

Declaration of Competing Interest

The authors declare that they have no known competing financial interests or personal relationships that could have appeared to influence the work reported in this paper.

Acknowledgements

This material is based upon work supported by the National Science Foundation under Grant No. 1936146. The authors also acknowledge the support for this work provided by the Auburn University Presidential Awards for Interdisciplinary Research Program.

Appendix A. Supplementary material

Supplementary data to this article can be found online at https://doi.org/10.1016/j.eurpolymj.2021.110307.

References

[1] H. Yasuda, C.E. Lamaze, L.D. Ikenberry, Permeability of solutes through hydrated polymer membranes. Part I. Diffusion of sodium chloride, Die, Makromol. Chem. 118 (1968) 19–35, https://doi.org/10.1002/macp.1968.021180102.
[2] H. Yasuda, A. Peterlin, C.K. Colton, K.A. Smith, E.W. Merrill, Permeability of solutes through hydrated polymer membranes. Part III. Theoretical background for the selectivity of dialysis membranes, Die, Makromol. Chem. 126 (1969) 177–186, https://doi.org/10.1002/macp.1969.021260120.
[3] J.G. Wijmans, R.W. Baker, The solution-diffusion model: a review, J. Membr. Sci. 107 (1995) 1–21, https://doi.org/10.1016/0376-7388(95)00102-i.
[4] A. Kusoglu, A.Z. Weber, New Insights into Perfluorinated Sulfonic-Acid Ionomers, Chem. Rev. 117 (2017) 987–1104, https://doi.org/10.1021/acs.chemrev.6b00159.
[5] J. Kamcev, B.D. Freeman, Charged Polymer Membranes for Environmental/Energy Applications, Annu. Rev. Chem. Biomol. 7 (2015) 1–23, https://doi.org/10.1146/annurev-chembioeng-080615-033533.
[6] G. Geise, M. Hickner, B. Logan, Ionic resistance and permselectivity tradeoffs in anion exchange membranes., Acs Appl Mater Inter. 5 (2013) 10294–301. https://doi.org/10.1021/am403207w.
[7] M. Galizia, D.R. Paul, B.D. Freeman, Liquid methanol sorption, diffusion and permeation in charged and uncharged polymers, Polymer 102 (2016) 281–291, https://doi.org/10.1016/j.polymer.2016.09.010.
[8] A.R. Crothers, R.M. Darling, D.I. Kushner, M.L. Perry, A.Z. Weber, Theory of Multicomponent Phenomena in Cation-Exchange Membranes: Part III. Transport in Vanadium Redox-Flow-Battery Separators, J. Electrochem. Soc. 167 (2020), 013549, https://doi.org/10.1149/1945-7111/ab6725.
[9] D.J. Miller, F.A. Houle, Energy and Environment Series, (2018) 341–385. https://doi.org/10.1039/9781788010313-00341.
[10] L.M. Robeson, H.H. Hwu, J.E. McGrath, Upper bound relationship for proton exchange membranes: Empirical relationship and relevance of phase separated blends, J Membrane Sci. 302 (2007) 70–77, https://doi.org/10.1016/j.memsci.2007.06.029.
[11] A. Heinzel, V.M. Barragán, A review of the state-of-the-art of the methanol crossover in direct methanol fuel cells, J. Power Sour. 84 (1999) 70–74, https://doi.org/10.1016/s0378-7753(99)00302-x.
[12] M.R. Singh, A.T. Bell, Design of an artificial photosynthetic system for production of alcohols in high concentration from CO 2, Energ. Environ. Sci. 9 (2015) 193–199, https://doi.org/10.1039/c5ee02783g.
[13] A. Berger, R.A. Segalman, J. Newman, Material requirements for membrane separators in a water-splitting photoelectrochemical cell, Energy Environ. Sci. (2014), https://doi.org/10.1039/C3EE43807D.
[14] S.M. Dischinger, S. Gupta, B.M. Carter, D.J. Miller, Transport of Neutral and Charged Solutes in Imidazolium-Functionalized Poly(phenylene oxide) Membranes for Artificial Photosynthesis, Ind. Eng. Chem. Res. 59 (2019) 5257–5266, https://doi.org/10.1021/acs.iecr.9b05628.
[15] B.M. Carter, B.M. Dobyns, B.S. Beckingham, D.J. Miller, Multicomponent transport of alcohols in an anion exchange membrane measured by in-situ ATR FTIR spectroscopy, Polymer 123 (2017), https://doi.org/10.1016/j.polymer.2017.06.070.
[16] X. Nie, M.R. Esopi, M.J. Janik, A. Asthagiri, Selectivity of CO(2) reduction on copper electrodes: the role of the kinetics of elementary steps., Angewandte Chemie Int Ed Engl. 52 (2013) 2459–62. https://doi.org/10.1002/anie.201208320.
[17] A. Loiudice, P. Lobaccaro, E.A. Kamali, T. Thao, B.H. Huang, J.W. Ager, R. Buonsanti, Tailoring Copper Nanocrystals towards C 2 Products in Electrochemical CO 2 Reduction, Angew. Chem. Int. Ed. 55 (2016) 5789–5792, https://doi.org/10.1002/anie.201601582.
[18] M. Krödel, B.M. Carter, D. Rall, J. Lohaus, M. Wessling, D.J. Miller, Rational Design of Ion Exchange Membrane Material Properties Limits the Crossover of CO 2 Reduction Products in Artificial Photosynthesis Devices, Acs Appl. Mater. Inter. 12 (2020) 12030–12042, https://doi.org/10.1021/acsami.9b21415.
[19] R.T. Chern, W.J. Koros, B. Yui, H.B. Hopfenberg, V.T. Stannett, Selective permeation of CO2 and CH4 through kapton polyimide: Effects of penetrant competition and gas-phase nonideality, J. Polym. Sci. Polym. Phys. Ed. 22 (1984) 1061–1084, https://doi.org/10.1002/pol.1984.180220610.
[20] B.S. Beckingham, N.A. Lynd, D.J. Miller, Monitoring multicomponent transport using in situ ATR FTIR spectroscopy, J. Membr. Sci. 550 (2018), https://doi.org/10.1016/j.memsci.2017.12.072.
[21] J.M. Kim, B.M. Dobyns, R. Zhao, B.S. Beckingham, Multicomponent transport of methanol and acetate in a series of crosslinked PEGDA-AMPS cation exchange membranes, J. Membr. Sci. (2020), 118486, https://doi.org/10.1016/j.memsci.2020.118486.
[22] N. Yan, D.R. Paul, B.D. Freeman, Water and ion sorption in a series of cross-linked AMPS/PEGDA hydrogel membranes, Polymer 146 (2018) 196–208, https://doi.org/10.1016/j.polymer.2018.05.021.
[23] K. Kabiri, S. Lashani, M.J. Zohuriaan-Mehr, M. Kheirabadi, Super alcohol-absorbent gels of sulfonic acid-contained poly(acrylic acid), J. Polym. Res. 18 (2010) 449–458, https://doi.org/10.1007/s10965-010-9436-y.
[24] A.C. Sagle, E.M.V. Wagner, H. Ju, B.D. McCloskey, B.D. Freeman, M.M. Sharma, PEG-coated reverse osmosis membranes: Desalination properties and fouling resistance, J. Membr. Sci. 340 (2009) 92–108, https://doi.org/10.1016/j.memsci.2009.05.013.
[25] H. Ju, A.C. Sagle, B.D. Freeman, J.I. Mardel, A.J. Hill, Characterization of sodium chloride and water transport in crosslinked poly(ethylene oxide) hydrogels, J. Membr. Sci. 358 (2010) 131–141, https://doi.org/10.1016/j.memsci.2010.04.035.
[26] H. Ju, B.D. McCloskey, A.C. Sagle, V.A. Kusuma, B.D. Freeman, Preparation and characterization of crosslinked poly(ethylene glycol) diacrylate hydrogels as fouling-resistant membrane coating materials, J. Membr. Sci. 330 (2009) 180–188, https://doi.org/10.1016/j.memsci.2008.12.054.
[27] L.J. Kirwan, P.D. Fawell, W. van Bronswijk, In Situ FTIR-ATR Examination of Poly (acrylic acid) Adsorbed onto Hematite at Low pH, Langmuir 19 (2003) 5802–5807, https://doi.org/10.1021/la027012d.
[28] H. Lin, E.V. Wagner, J.S. Swinnea, B.D. Freeman, S.J. Pas, A.J. Hill, S. Kalakkunnath, D.S. Kalika, Transport and structural characteristics of crosslinked poly(ethylene oxide) rubbers, J. Membr. Sci. 276 (2006) 145–161, https://doi.org/10.1016/j.memsci.2005.09.040.
[29] B.M. Dobyns, J.M. Kim, B.S. Beckingham, Multicomponent transport of methanol and sodium acetate in poly(ethylene glycol) diacrylate membranes of varied fractional free volume, Eur. Polym. J. 134 (2020), 109809, https://doi.org/10.1016/j.eurpolymj.2020.109809.
[30] F.G. Helfferich, Ion Exchange, Dover, 1995.
[31] G.M. Geise, B.D. Freeman, D.R. Paul, Characterization of a sulfonated pentablock copolymer for desalination applications, Polymer 51 (2010) 5815–5822, https://doi.org/10.1016/j.polymer.2010.09.072.
[32] S. Lindenbaum, C.F. Jumper, G.E. Boyd, Selectivity Coefficient Measurements with Variable Capacity Cation and Anion Exchangers, J. Phys. Chem. 63 (1959) 1924–1929, https://doi.org/10.1021/j150581a031.
[33] L.E. Karlsson, P. Jannasch, B. Wesslén, Preparation and Solution Properties of Amphiphilic Sulfonated Acrylamide Copolymers, Macromol. Chem. Physic. 203 (2002) 686–694, https://doi.org/10.1002/1521-3935(20020301)203:4<686::aid-macp686>3.0.co;2-c.
[34] N.A. Choudhury, A.K. Shukla, S. Sampath, S. Pitchumani, Cross-Linked Polymer Hydrogel Electrolytes for Electrochemical Capacitors, J. Electrochem. Soc. 153 (2006) A614, https://doi.org/10.1149/1.2164810.
[35] T. Borjigin, F. Sun, J. Zhang, K. Cai, H. Ren, G. Zhu, A microporous metal–organic framework with high stability for GC separation of alcohols from water, Chem. Commun. 48 (2012) 7613–7615, https://doi.org/10.1039/c2cc33023g.
[36] E.R. Nightingale, Phenomenological Theory of Ion Solvation. Effective Radii of Hydrated Ions, J. Phys. Chem. 63 (1959) 1381–1387, https://doi.org/10.1021/j150579a011.
[37] R. Caminiti, P. Cucca, M. Monduzzi, G. Saba, G. Crisponi, Divalent metal–acetate complexes in concentrated aqueous solutions. An x-ray diffraction and NMR spectroscopy study, J. Chem. Phys. 81 (1984) 543–551, https://doi.org/10.1063/1.447336.
[38] Hitoshi. Ohtaki, Tamas. Radnai, Structure and dynamics of hydrated ions, Chem Rev. 93 (1993) 1157–1204. https://doi.org/10.1021/cr00019a014.
[39] B.M. Dobyns, J.M. Kim, J. Li, Z. Jiang, B.S. Beckingham, Multicomponent transport of alcohols in Nafion 117 measured by in situ ATR FTIR spectroscopy, Polymer (2020), 123046, https://doi.org/10.1016/j.polymer.2020.123046.
[40] B. Pan, B. Xing, Competitive and Complementary Adsorption of Bisphenol A and 17α-Ethinyl Estradiol on Carbon Nanomaterials, J. Agr. Food. Chem. 58 (2010) 8338–8343, https://doi.org/10.1021/jf101346e.
[41] K.A. Thompson, R. Mathias, D. Kim, J. Kim, N. Rangnekar, J.R. Johnson, S.J. Hoy, I. Bechis, A. Tarzia, K.E. Jelfs, B.A. McCool, A.G. Livingston, R.P. Lively, M.G. Finn, N-Aryl-linked spirocyclic polymers for membrane separations of complex hydrocarbon mixtures, Sci. New York N Y. 369 (2020) 310–315, https://doi.org/10.1126/science.aba9806.
[42] V.N. Afanas'ev, Solvation of Electrolytes and Nonelectrolytes in Aqueous Solutions, J Phys Chem B. 115 (2011) 6541–6563. https://doi.org/10.1021/jp1108834.
[43] G.M. Geise, D.R. Paul, B.D. Freeman, Fundamental water and salt transport properties of polymeric materials, Prog. Polym. Sci. 39 (2014) 1–42, https://doi.org/10.1016/j.progpolymsci.2013.07.001.